Topological signatures in Kerr-Sen AdS black hole thermodynamics

Mohd Rehan[1†] Md Sabir Ali[2,3,4‡] Sushant G. Ghosh[1,5§]

[1]Centre for Theoretical Physics, Jamia Millia Islamia, New Delhi 110025, India
[2]Department of Physics, Mahishadal Raj College, Purba Medinipur, West Bengal 721628, India
[3]Institute of Theoretical Physics & Research Center of Gravitation, Lanzhou University, Lanzhou 730000, China
[4]School of Physical Science and Technology, Lanzhou University, Lanzhou 730000, China
[5]Astrophysics and Cosmology Research Unit, School of Mathematics, Statistics and Computer Science, University of KwaZulu-Natal, Private Bag X54001, Durban 4000, South Africa

Abstract: Black hole thermodynamics and topology have emerged as a robust foundation for a coordinate-independent understanding of phase transitions. Using both Duan's topological current theory and a novel complex residue method, we conduct a topological study of the Kerr-Sen AdS black hole arising in heterotic string theory. Specifically, we identify the zero points corresponding to on-shell black hole states and calculate their winding numbers to determine the global topological charge by constructing the generalized off-shell free energy and examining the corresponding vector field in a parametric space. Our analysis reveals that the Kerr-Sen AdS black hole exhibits three distinct thermodynamic phases—small, intermediate, and large black hole branches—characterized by critical points with winding numbers $+1$, -1, and $+1$, respectively, culminating in a total topological charge $W=+1$. Significantly, this topological number remains invariant under variations of the dilaton charge parameter, indicating that the dilaton field does not alter the fundamental topological class established for Kerr-AdS and RN-AdS black holes. However, the rotation parameter proves crucial in determining the phase structure and the emergence of multiple critical points. We systematically examine three limiting configurations: the full Kerr-Sen AdS spacetime, the GMGHS AdS limit ($a=0$), and the asymptotically flat Kerr-Sen case ($\Lambda=0$). The GMGHS AdS black hole yields a vanishing total topological charge, with winding numbers $+1$ and -1 canceling each other, while the Kerr-Sen black hole ($\Lambda=0$) similarly exhibits $W=0$ despite possessing two distinct phase branches. Furthermore, we propose a novel approach by analytically continuing the thermodynamic characterization to the complex plane. The resulting complex function, derived from the off-shell Gibbs free energy, possesses isolated singular points whose residues directly encode the winding numbers. Our results indicate that topology offers profound insights into black hole phase transitions, with potential implications for understanding holographic dualities.

Keywords: Kerr-Sen black hole, thermodynamic topology, phase transition, Duan's topological current, complex residue method, AdS spacetime

DOI: 10.1088/1674-1137/ae9278 **CSTR:** 32044.14.ChinesePhysicsC.50115111

I. INTRODUCTION

Black holes have evolved from exact solutions of Einstein's general relativity (GR) into observationally accessible astrophysical objects, with the LIGO/Virgo collaborations detecting gravitational waves from black hole mergers [1, 2] and the Event Horizon Telescope (EHT) providing the first direct images of the black hole shadows of M87* and Sgr A* [3, 4]. The EHT and LIGO/Virgo observations have opened a window onto an era of precision strong gravity, enabling exceptional tests of gravitational theories in the extreme-curvature regime.

The current decade is regarded as the dawn of precision strong gravity. Observational data from LIGO/Virgo/LISA and EHT/ngEHT are being used to test, in particular, the true nature of astrophysical black holes. The ability to see the unseen and to hear echoes from the darkest regions of the universe is now within reach. Hence, gravitational-wave detections of black hole mergers through the ringdown phase and shadow imaging of black holes through electromagnetic observations are expected to provide previously inaccessible information about the strong-field regime of gravity. Theoretically, it is anticipated that exploring black hole topology to un-

Received 20 July 2026; Accepted 29 July 2026; Accepted manuscript online 30 July 2026

† E-mail: rk1958227@gmail.com
‡ E-mail: alimd.sabir3@gmail.com
§ E-mail: sghosh2@jmi.ac.in

©2026 Chinese Physical Society and the Institute of High Energy Physics of the Chinese Academy of Sciences and the Institute of Modern Physics of the Chinese Academy of Sciences and IOP Publishing Ltd. All rights, including for text and data mining, AI training, and similar technologies, are reserved.

cover the true nature of gravity can be achieved *vis-à-vis* knowledge of the topological structure of light rings, timelike circular orbits [5, 6], and thermodynamic properties [7–9].

The thermodynamic interpretation of black holes stands as one of the most profound conceptual developments in theoretical physics. The four laws of black hole mechanics [10] and Hawking radiation [11, 12] indicate that black holes possess temperature and entropy, thereby establishing a fundamental connection among gravitation, quantum mechanics, and thermodynamics. The thermodynamic analogy arises naturally in anti-de Sitter (AdS) spacetimes, where black holes exhibit rich phase structures reminiscent of van der Waals liquid-gas systems [13]. The Hawking-Page phase transition between thermal AdS space and large Schwarzschild-AdS black holes [13] marked a remarkable milestone, establishing black hole thermodynamics as a fruitful arena for exploring gauge/gravity dualities. The phase-transition behavior of AdS black holes and their topological classification using the generalized off-shell free-energy approach provide valuable insights into the fundamental nature of gravity [14–18].

In recent years, the investigation of black hole thermodynamics has been revolutionized by the application of topological methods. Inspired by Duan's ϕ-mapping topological current theory [19–21], Wei, Liu, and Mann [7, 22] introduced a novel framework in which black hole solutions are treated as topological defects in a thermodynamic parameter space. In this approach, they construct a generalized off-shell free energy and study an associated vector field. The zero points of this vector field correspond exactly to on-shell black hole states and are assigned winding numbers, or topological charges. The sum of these winding numbers yields a topological number that characterizes the entire system. Remarkably, this number remains unchanged under smooth variations of the thermodynamic parameters, making it a universal property. The same approach has also been used to study timelike circular orbits around stationary black holes [22].

The topological framework has been systematically applied to a diverse range of black hole solutions. Studies have explored vacuum AdS solutions in classical GR [23], regular black holes including Bardeen and Hayward-AdS solutions [24, 25], Einstein-Gauss-Bonnet AdS black holes [26], Lovelock gravity [27], and Born-Infeld AdS black holes [28]. Rotating spacetimes [29, 30] have revealed that spin significantly influences topological classifications, with Kerr-Sen-AdS black holes exhibiting superentropic behavior [31]. The thermodynamics of Kerr-Sen-AdS black holes has been further investigated within the restricted phase-space formalism [32–34].

Similarly, Fang [25] proposed a complementary approach based on complex residue techniques: by analytically continuing thermodynamic functions into the complex plane, one can construct characteristic functions whose isolated singularities correspond to thermodynamic defects. It turns out that the residues at these poles encode winding numbers, providing a mathematically elegant method that reproduces and extends Duan's topological approach. Recent work has extended this method to the restricted phase-space thermodynamics of Kerr-Sen-AdS black holes [35]. Establishing the correspondence between Duan's topological current method and residue techniques helps distinguish the creation and annihilation profiles of black hole phase transitions near critical points. Such methods have been employed for a class of black hole solutions in which the creation/annihilation behavior and the critical points are categorized through coefficient analysis of the Laurent series of the complexified off-shell Gibbs free energy.

Of particular interest, in a more recent version of the geometric interpretation [36–39], black hole phase structures are probed through topological classifications based on Duan's ϕ-mapping topological current and the corresponding winding number defined in an auxiliary parameter space [7, 8]. When the thermal phase behavior of black hole solutions is treated as a set of topological defects, these solutions can be classified into three distinct categories, each corresponding to a different topological charge and associated topological number. Hence, the classification of black hole solutions as topological defects, together with the investigation of phase-transition behavior at critical points through a temperature-dependent function, broadly categorizes topological charges into two distinct subclasses: one corresponding to conventional critical points and the other associated with novel phase transitions.

Despite extensive investigation, the topology of AdS black holes still remains elusive. The rationale for such studies lies in the fact that topological numbers possess universal features independent of the parameters characterizing the black hole. Hence, topology plays a pivotal role in deciphering the nature of black holes and gravitational theory. Owing to its versatility and naturalness, the topological framework has gained rapid acceptance because of its conceptual simplicity and adaptability to diverse gravitational theories. Consequently, ever since its inception, topological numbers and their classifications have been explored in a wide range of known black hole solutions, e.g., vacuum/electro-vacuum AdS solutions in classical general relativity [23], regular AdS black hole solutions [24, 25, 40], Einstein-Gauss-Bonnet AdS black holes [41], black holes in Lovelock gravity [27], and Born-Infeld AdS black holes [28]. Later, such studies were extended to rotating spacetimes [29, 30, 34]. In a recent work, a systematic topological classification of rotating accelerating black holes and their AdS extensions was carried out for both neutral and charged cases. The ana-

lysis revealed that the acceleration parameter and the negative cosmological constant each independently increase the topological number by one unit; however, when both effects are present simultaneously, their contributions cancel each other, resulting in no net change in the topological number [42]. Since the topological classification of rotating AdS black holes is still in its early stages, it deserves deeper analysis. Furthermore, rotating AdS black holes are fundamentally connected to gauge/gravity dualities, as they shed light on the nature of quantum gravity. These considerations motivate us to study the thermodynamic topology of Kerr-Sen AdS black holes in their own right, as it provides a global, coordinate-independent framework for a basic understanding of black hole thermodynamics during phase transitions, especially in light of its emergence from string theory.

Motivated by this, we address the above questions through a topological analysis of Kerr-Sen AdS black holes. The Kerr-Sen AdS black hole represents a rotating string-theory black hole containing a non-trivial dilaton field, whose thermodynamic topology has not been systematically analyzed using both Duan's topological current formalism and the complex residue method. Unlike Kerr-AdS and RN-AdS black holes, the Kerr–Sen AdS spacetime possesses an additional dilaton parameter. Our analysis demonstrates that although the dilaton modifies the thermodynamic quantities locally, it does not alter the global topological class, thereby revealing a remarkable universality of thermodynamic topology. We perform a systematic investigation of three physically important configurations —the full Kerr-Sen AdS spacetime, the GMGHS AdS limit ($a=0$), and the asymptotically flat Kerr-Sen limit ($\Lambda=0$). Their topological relations have not previously been analyzed within a unified framework. We further compute the angular deflection of the unit vector field to characterize the topological charge of each critical point. Additionally, we apply the complex residue technique to this system, demonstrating its ability to reproduce and extend the topological classification while offering new insights into the nature of critical points. The equivalence between Duan's topological current method and the complex residue formulation for Kerr-Sen black holes ensures the mathematical advantages of the residue approach in identifying creation and annihilation points of thermodynamic defects.

The organization of the paper is as follows. In Section II, we briefly review Kerr-Sen AdS black holes and their thermodynamic quantities. Using the definition of the off-shell Gibbs free energy, we identify the topological charges and their possible classifications based on Duan's topological mapping theory. In Section III, we analyze our results in the context of complex residue techniques by defining a characteristic function constructed from the off-shell Gibbs free energy of a Kerr-Sen black hole. In Section IV, we discuss our results and conclude the paper.

II. KERR-SEN ADS BLACK HOLE AND ITS TOPOLOGY

The Kerr-Sen AdS black hole is a rotating black hole spacetime arising from the low-energy effective action of heterotic string theory and incorporating both a dilaton field and a negative cosmological constant. It generalizes the original Kerr-Sen spacetime [43] to asymptotically anti-de Sitter backgrounds. The Kerr-Sen AdS black hole is particularly significant in the context of black hole thermodynamics, as the presence of the cosmological constant introduces a rich phase structure similar to that of van der Waals liquid-gas systems. At the same time, its string-theoretic origin provides a natural framework for exploring corrections to Einstein gravity and their implications for gauge/gravity duality. In the usual Boyer-Lindquist coordinates, the Kerr-Sen AdS metric takes the form [32, 34, 44]

$$\begin{aligned} \mathrm{d}s^2 = &-\frac{\Delta_r}{\rho^2}\left(\mathrm{d}t-\frac{a\sin^2\theta}{\Xi}\mathrm{d}\phi\right)^2+\frac{\rho^2}{\Delta_r}\mathrm{d}r^2+\frac{\rho^2}{\Delta_\theta}\mathrm{d}\theta^2 \\ &+\frac{\sin^2\theta\Delta_\theta}{\rho^2}\left(a\,\mathrm{d}t-\frac{r^2+2br+a^2}{\Xi}\mathrm{d}\phi\right)^2, \end{aligned} \tag{1}$$

where

$$\rho^2 = r^2+2br+a^2\cos^2\theta, \tag{2}$$

$$\Delta_r = \left(r^2+2br+a^2\right)\left(1+\frac{r^2+2br}{\ell^2}\right)-2Gmr, \tag{3}$$

$$\Xi = 1-\frac{a^2}{\ell^2}, \qquad \Delta_\theta = 1-\frac{a^2}{\ell^2}\cos^2\theta. \tag{4}$$

$$M = \frac{m}{\Xi^2}, \quad J = \frac{ma}{\Xi^2}, \quad Q = \frac{q}{\Xi}, \tag{5}$$

where the mass parameter m can be obtained from the condition $\Delta_r(r=r_h)=0$ with r_h denoting the radius of the event horizon. Consequently, the mass M and angular momentum J can be expressed in terms of a, r_h, G. The thermodynamic quantities associated with the above solution Eq. (1) can be derived using the standard methods, and are given by the following explicit expressions [32, 34]

$$M = \frac{1}{2\Xi^2 G r_h}\left(r_h^2+2br_h+a^2\right)\left(1+\frac{r_h^2+2br_h}{\ell^2}\right), \tag{6}$$

$$J=\frac{a\left(r_h^2+2br_h+a^2\right)}{2\Xi^2 G r_h}\left(1+\frac{r_h^2+2br_h}{\ell^2}\right). \tag{7}$$

The corresponding expressions for Kerr-AdS black holes are obtained when $b=0$ [33],

$$M=\frac{1}{2\Xi^2 G r_h}\left(r_h^2+a^2+\frac{r_h^4}{\ell^2}+\frac{a^2 r_h^2}{\ell^2}\right), \tag{8}$$

$$J=\frac{a}{2\Xi^2 G r_h}\left(r_h^2+a^2+\frac{r_h^4}{\ell^2}+\frac{a^2 r_h^2}{\ell^2}\right). \tag{9}$$

The rest of the thermodynamic quantities can be written as

$$S=\frac{\pi\left(r_h^2+2br_h+a^2\right)}{G\Xi}, \tag{10}$$

$$\Omega=\frac{a\Xi}{r_h^2+2br_h+a^2}+\frac{a}{\ell^2}, \tag{11}$$

$$\Phi=\frac{qr_h}{r_h^2+2br_h+a^2}. \tag{12}$$

Here m, a, and b are, respectively, the mass, the spin parameter, and the dilaton charge. It is presumed that the presence of the dilaton charge parameter b modifies the expressions for entropy (S), angular velocity (Ω), and the electric potential (Φ). The parameter b is expressed as $b=q^2/2m$ where q is the electric charge of the black hole. In the extended phase space of black hole mechanics, the cosmological constant is treated as the thermodynamic pressure through the relation

$$P=-\frac{\Lambda}{8\pi}=\frac{3}{8\pi\ell^2}.$$

The volume conjugate to the pressure is defined as

$$V=\left(\frac{\partial M}{\partial P}\right)_{S,J,Q}.$$

With these definitions of the pressure and volume, we write the first law of the Kerr-Sen AdS black hole mechanics as

$$\mathrm{d}M=T\,\mathrm{d}S+\Omega\,\mathrm{d}J+\Phi\,\mathrm{d}Q+P\mathrm{d}V.$$

The corresponding Smarr relation can be obtained using scaling arguments.

$$M=2TS+2\Omega J+\Phi\,\mathrm{d}Q-2PV.$$

The extended phase-space thermodynamics of the Kerr-Sen AdS black hole exhibits van der Waals-like phase transition behavior near the critical points. This feature can be used to define the topology of thermodynamic defects for Kerr-Sen AdS black holes.

With the expressions for the thermodynamic quantities in hand, we are now ready to investigate the topological number of the four-dimensional Kerr-Sen AdS black hole. As discussed in Refs. [33, 34], one may first introduce the generalized off-shell free energy as

$$\mathcal{F}=M-\frac{S}{\tau}, \tag{13}$$

for a black hole system with mass M and entropy S, where τ is an additional variable that can be interpreted as the inverse temperature of the cavity surrounding the black hole. Only when $\tau=1/T$ does the generalized free energy become on-shell.

As reported in Refs. [28, 34], a two-dimensional vector $\phi=(\phi^{r_h},\phi^{\Theta})$ is conventionally written as

$$\phi=\left(\frac{\partial\mathcal{F}}{\partial r_h},-\cot\Theta\csc\Theta\right), \tag{14}$$

where the parameter $0\le\Theta\le+\infty$ is introduced for convenience and intuitive interpretation. The component ϕ^{Θ} diverges at $\Theta=0,\pi$, and the direction of the vector points outward at these points. Furthermore, as discussed in Ref. [22], the extremal points of the generalized free energy landscape exactly correspond to the on-shell black holes, so the zero of the component ϕ^{r_h} exactly corresponds to the black hole solution. The condition $\phi^{\Theta}=0$ then yields $\Theta=\pi/2$.

According to Duan's ϕ-mapping topological current theory, a topological current can be defined as [19, 21, 45]

$$j^{\mu}=\frac{1}{2\pi}\epsilon^{\mu\nu\rho}\epsilon_{ab}\partial_{\nu}n^{a}\partial_{\rho}n^{b},\quad \mu,\nu,\rho=0,1,2, \tag{15}$$

where $\partial_{\nu}=\partial/\partial x^{\nu}$ and $x^{\nu}=(\tau,\, r_h,\, \Theta)$. The unit vector n is given by $n=(n^{r},n^{\Theta})$, where $n^{r}=\phi^{r_h}/\|\phi\|$ and $n^{\Theta}=\phi^{\Theta}/\|\phi\|$. Once the topological current Eq. (15) is constructed, one can readily show that it is conserved; hence, the continuity equation $\partial_{\mu}j^{\mu}=0$ holds identically due to the underlying symmetry. It is further shown that the topological current j^{μ} is a δ-function of the field configuration [21, 45, 46]

$$j^{\mu}=\delta^{2}(\phi)J^{\mu}\left(\frac{\phi}{x}\right), \tag{16}$$

where the quantity $J^{\mu}(\phi/x)$ denotes the three-dimension-

al Jacobian, given by $\epsilon^{ab}J^{\mu}(\phi/x)=\epsilon^{\mu\nu\rho}\partial_{\nu}\phi^{a}\partial_{\rho}\phi^{b}$. It can be readily shown that the topological current j^{μ} vanishes identically except at points where $\phi^{a}(x_i)=0$. This allows us to express the topological number W in a given parametric region Σ as:

$$W=\int_{\Sigma}j^{0}\mathrm{d}^{2}x=\sum_{i=1}^{N}\beta_i\eta_i=\sum_{i=1}^{N}w_i, \tag{17}$$

where β_i is the positive Hopf index that counts the number of loops of the vector field ϕ^{a} in ϕ-space, whereas x^{μ} is evaluated around the zero points z_i. The parameter $\eta_i=\mathrm{sign}(J^{0}(\phi/x)_{z_i})=\pm1$ represents the Brouwer degree, and w_i is the winding number associated with the ith zero point of ϕ contained in the parameter region Σ. It is worth noting that if two loops, Σ_1 and Σ_2, surround the same zero point of ϕ, then they have the same winding number. On the other hand, if there is no zero point in the enclosed region, one can have $W=0$. The values of w_i play a crucial role in determining the local thermodynamic stability of a black hole. In this regard, one may also speculate that the positive or negative heat capacity of a black hole state corresponds to the winding number $w=+1$ or $w=-1$, respectively, thereby reflecting the local stability or instability of the black hole state. As a specific rule for determining the difference between the numbers of thermally stable and unstable phases at a given off-shell configuration, we need to evaluate the global topological number W. Hence, W is a characteristic feature of each black hole system and serves as a classification parameter.

A. Topological classes of Kerr-Sen AdS black hole

In this section, we study the topology of the Kerr-Sen AdS black hole [34]. From the results presented in Eq. (13), one can readily obtain the generalized free energy

$$\mathcal{F}=\frac{3\left(a^2+2br+r^2\right)\left[3\tau+\pi r\left(16a^2P\pi-6+16bP\tau+8Pr\tau\right)\right]}{2Gr\tau(3-8a^2P\pi)^2} \tag{18}$$

of the Kerr-Sen AdS black hole. The components of the vector ϕ can then be computed as

$$\phi^{r_h}=\frac{3}{2G_N(3-8a^2P\pi)^2\tau}\left\{\pi\left(32a^2P\pi r-12r-12b\right)+\tau\left[\pi\left(32b^2P+8a^2P+64bPr+24Pr^2\right)+\frac{3(r^2-a^2)}{r^2}\right]\right\}, \tag{19}$$

$$\phi^{\Theta}=-\cot\Theta\csc\Theta. \tag{20}$$

By solving the equation $\phi^{r_h}=0$, one can obtain a solution represented by a curve on the $r_h-\tau$ plane. For the four-dimensional Kerr-Sen AdS black hole, one obtains

$$\tau=\frac{4\pi(3-8a^2P\pi)r^3}{a^2(8P\pi r^2-3)+r^2(3+32b^2P\pi+64bP\pi r+24P\pi r^2)}. \tag{21}$$

The expressions given in Eq. (18), Eq. (19), and Eq. (21) reduce to the corresponding expressions for the four-dimensional Kerr-AdS case when the dilation charge vanishes. From a topological perspective, it is well known that if a closed contour encloses a critical point, it carries a nonzero topological charge; otherwise, the topological charge vanishes. To calculate the topological charge, we construct three closed contours, C_1, C_2, and C_3, parametrized by $\vartheta\in(0,2\pi)$ as

$$\begin{cases} r=X\cos\vartheta+r_0, \\ \theta=Y\sin\vartheta+\dfrac{\pi}{2}. \end{cases} \tag{22}$$

We choose $(X,Y,r_0)=(0.05,0.08,0.10122)$ for contour C_1, $(X,Y,r_0)=(0.08,0.08,0.3408)$ for contour C_2, and $(X,Y,r_0)=(0.08,0.08,0.864029)$ for contour C_3. To better understand the behavior of the vector field along each contour, we introduce a new quantity that quantifies the deflection of the vector field as–

$$\Omega(\vartheta)=\int_{0}^{\vartheta}\epsilon_{ab}\,n^{a}\,\partial_{\vartheta}n^{b}\,\mathrm{d}\vartheta, \tag{23}$$

where n^{a} denotes a unit vector field and ϵ_{ab} is the two-dimensional Levi-Civita symbol. The topological charge is then given by

$$Q=\frac{1}{2\pi}\Omega(2\pi). \tag{24}$$

Figure 1 shows the zero points of the vector field in a region of the r_h–Θ plane for the Kerr-Sen AdS black hole with parameters $a=0.08$ and $b=0.01$ at constant pressure P_0. The blue arrows represent the vector field. The zero points, ZP_1, ZP_2, and ZP_3, marked by red dots, are located at $(r_h,\Theta)=(0.10122,\pi/2)$, $(0.3408,\pi/2)$, and $(0.864029,\pi/2)$, respectively. The contours C_1, C_2, and C_3 are constructed to enclose these zero points. Consequently, the winding numbers for the contours C_1 (red solid), C_2 (black dashed), and C_3 (blue solid) are identi-

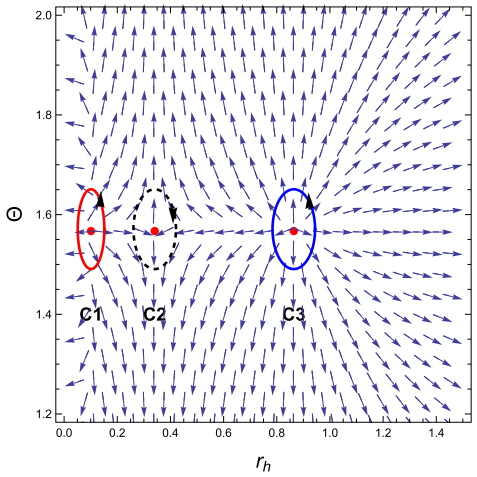


Fig. 1. (color online) The plot shows the unit vector field n on the r_h–Θ plane for a four-dimensional Kerr-Sen AdS black hole with $\tau = 3.3$ and $a = 0.08$. The zero points (ZPs), marked by red dots, are located at $(r_h, \Theta) = (0.1012204, \pi/2)$, $(0.34086, \pi/2)$, and $(0.86402, \pi/2)$. The contours C_1, C_2, and C_3 surrounding these zero points have winding numbers $w_1 = 1$, $w_2 = -1$, and $w_3 = 1$, respectively. Their sum defines the total topological charge $W = 1$.

fied as $w_1 = +1$, $w_2 = -1$, and $w_3 = +1$, respectively. For the global topological number, we obtain $W = w_1 + w_2 + w_3 = 1$. This feature exactly mimics the RN-AdS and Kerr-AdS cases in four dimensions, for which the global topological number is +1 [7, 30]. Thus, we infer that, for certain parameter values, the Kerr-Sen AdS black hole has the same geometric topology and belongs to the same topological class as these solutions in terms of thermodynamic topology. However, the topological number of the Schwarzschild-AdS black hole is 0; hence, we infer that the rotation and dilaton charge parameters play an important role in determining the topological number for Kerr-Sen AdS black holes.

The zero points ϕ^{r_h} in the $r_h - \tau$ plane are depicted in Fig. 2 for the fixed values of the rotation parameter, dilaton charge, and pressure, namely $a = 0.08$, $b = 0.01$, and $P = 0.1193$. For these values of a, b, and P, we have two inverse critical temperatures, $\tau_{c1} = 2.4903$ and $\tau_{c2} = 3.60951$, which characterize the phase transition behavior. The parameter τ_{c1} corresponds to the creation point, whereas τ_{c2} corresponds to the annihilation point. As shown in Fig. 2, there is one large black hole branch for $\tau < \tau_{c1}$, three branches for $\tau_{c1} < \tau < \tau_{c2}$, and one small black hole branch for $\tau > \tau_{c2}$.

For the contours C_1, C_2, and C_3, we plot $\Omega(\vartheta)$ in Fig. 3. The contours C_1 and C_3 evolve in the positive (anticlockwise) Ω direction, whereas the contour C_2 evolves in the negative (clockwise) Ω direction. This difference arises from their orientations, which produce winding numbers (or topological charges) of opposite signs. This indicates distinct topological properties for different ther-

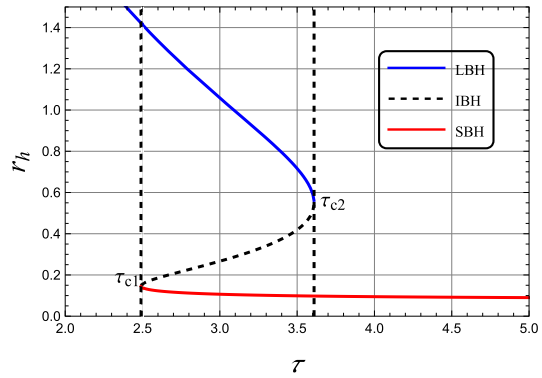


Fig. 2. (color online) The behavior of the zero points of ϕ^{r_h} in the $r_h - \tau$ plane for the Kerr-Sen AdS black hole is shown. The blue solid, black dashed, and red solid curves correspond to the large black hole (LBH), intermediate black hole (IBH), and small black hole (SBH) branches, respectively, for the Kerr–Sen AdS black hole with $a = 0.08$, $b = 0.01$, and $P = 0.1193$. Two critical temperatures, $\tau_{c1} = 2.4903$ and $\tau_{c2} = 3.60951$, characterize the phase transitions.

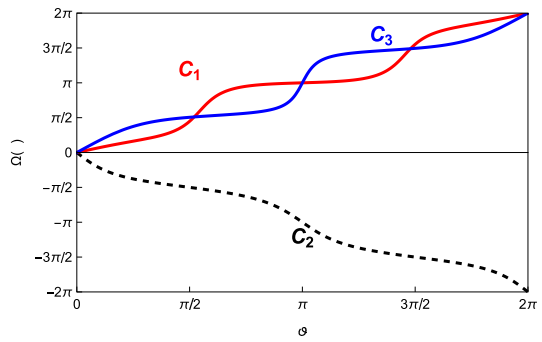


Fig. 3. (color online) Plot of the behavior of Ω as a function of ϑ for the contours C_1 (red solid curve), C_2 (black dashed curve), and C_3 (blue solid curve) for the Kerr-Sen AdS black hole.

modynamic phases of black holes. The fact that the contours remain well separated and do not overlap shows that the zero points are topologically protected. As a result, one type of phase transition behavior cannot smoothly evolve into another. Any transition between them requires the creation or annihilation of a zero point, indicating a topological phase transition of the black hole.

Accordingly, for the contours C_1 and C_3, $\Omega(\vartheta)$ increases monotonically and approaches 2π at $\vartheta = 2\pi$. Therefore, the topological charge associated with the critical points CP_1 and CP_3 is

$$Q_{\mathrm{CP}_1} = Q_{\mathrm{CP}_3} = +1, \tag{25}$$

and hence corresponds to the generation of topological charges on the contours. Furthermore, for the contour C_2, $\Omega(\vartheta)$ decreases monotonically and approaches -2π at $\vartheta = 2\pi$. Therefore, the topological charge associated with

the critical point CP_2 is

$$Q_{CP_2} = -1. \tag{26}$$

There is one annihilation point in this case. According to our classification, the presence of three critical points implies that the system admits three distinct thermodynamic phases, namely small, intermediate, and large black holes. Each critical point marks a first-order phase transition between two neighboring phases. Consequently, the system undergoes small–intermediate and intermediate–large black hole phase transitions in different regions of the parameter space, resulting in a rich and complex phase structure. The corresponding charges are denoted by Q_{CP_1}, Q_{CP_2}, and Q_{CP_3}, wherein the total charge is encoded as

$$Q_{tot} = Q_{CP_1} + Q_{CP_2} + Q_{CP_3} = 1. \tag{27}$$

The plot in Fig. 4 shows the behavior of the unit vector field n in the parametric space (r_h, Θ) for four-dimensional GMGHS charged black holes in AdS spacetime at inverse temperature $\tau = 2$ in the limit of a vanishing rotation parameter ($a = 0$). The ZPs enclosed by the contours are marked by red dots and are located at $(r_h, \Theta) = (0.16417, \pi/2)$ for C_1 and $(1.903549, \pi/2)$ for C_2. Depending on the orientations of the contours C_1 and C_2,

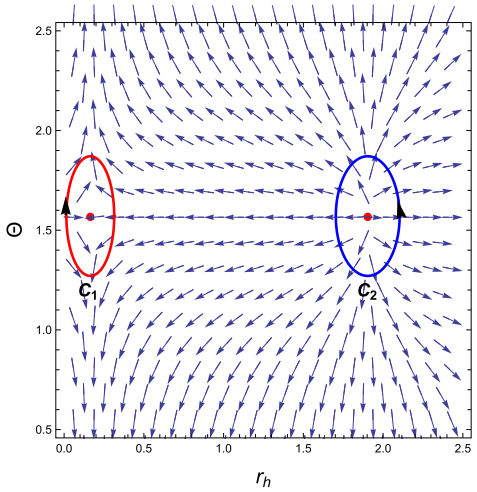


Fig. 4. (color online) The plot shows the unit vector field n on the r_h-Θ plane for four-dimensional Gibbons-Maeda-Garfinkle-Horowitz-Strominger (GMGHS) charged black holes in AdS spacetime with $\tau = 2$, when the rotation is switched off ($a = 0$). The zero points (ZPs), marked by red dots, are located at $(r_h, \Theta) = (0.16417, \pi/2)$ and $(1.903549, \pi/2)$. The orientations of the contours C_1 and C_2 are clockwise and anticlockwise, corresponding to the topological charges $Q_{c_1} = -1$ and $Q_{c_2} = +1$, respectively. The total topological charge is $Q_{total} = 0$.

we define the topological charges as $Q_{c_1} = -1$ and $Q_{c_2} = +1$, respectively, so that the total topological charge is $Q_{total} = 0$. To examine how the black hole evolves, we plot in Fig. 5 the zero points of ϕ^{r_h} in the parameter space (r_h, τ) for the parameter values $a = 0$, $b = 0.01$, and $P = 0.1193$. In this case, we obtain only one inverse critical temperature, $\tau_c = 3.6$, characterizing the phase transition behavior from the small black hole phase to the large black hole phase. Such phase transitions are absent in charged AdS black holes, which exhibit three distinct phases: SBH, IBH, and LBH.

For the two branches of the extended phase-space thermodynamics, we obtain the small and large black hole phases with winding numbers ("$w = +1$") and ("$w = -1$"), respectively, (the sign convention is referred in Table 1). when the spin parameter is set to zero. The values of the topological charges obtained from the integrals are shown in Fig. 6. Consequently, for the parameter values $a = 0$, $b = 0.01$, and $P = 0.1193$, we have a vanishing total topological charge, $Q_{total} = 0$, resulting from the

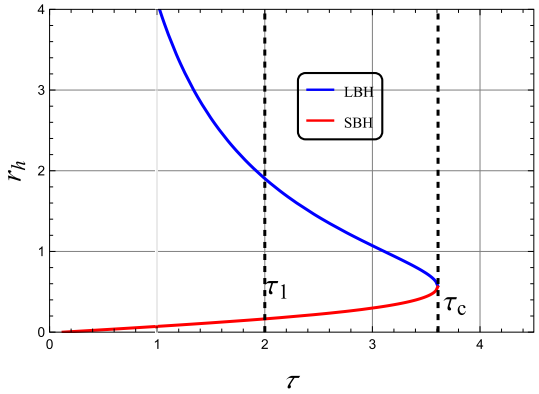


Fig. 5. (color online) The plot shows the behavior of the stable and unstable branches of the GMGHS AdS black hole phases, represented by the blue and red curves, respectively, for $a = 0$, $b = 0.01$, and $P = 0.1193$.

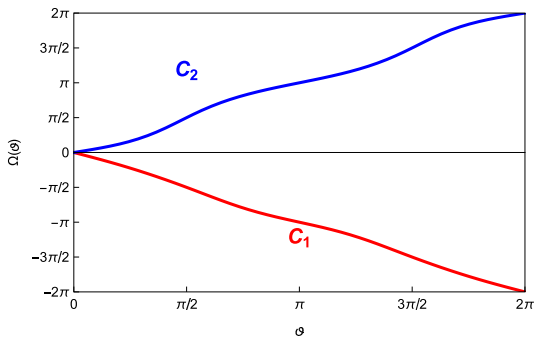


Fig. 6. (color online) The plot shows the behavior of Ω as a function of ϑ for the contours C_1 (red solid curve) and C_2 (blue solid curve), with $a = 0$, $b = 0.01$, and $P = 0.1193$. The blue and red curves correspond to the large black hole (LBH) and small black hole (SBH), respectively.

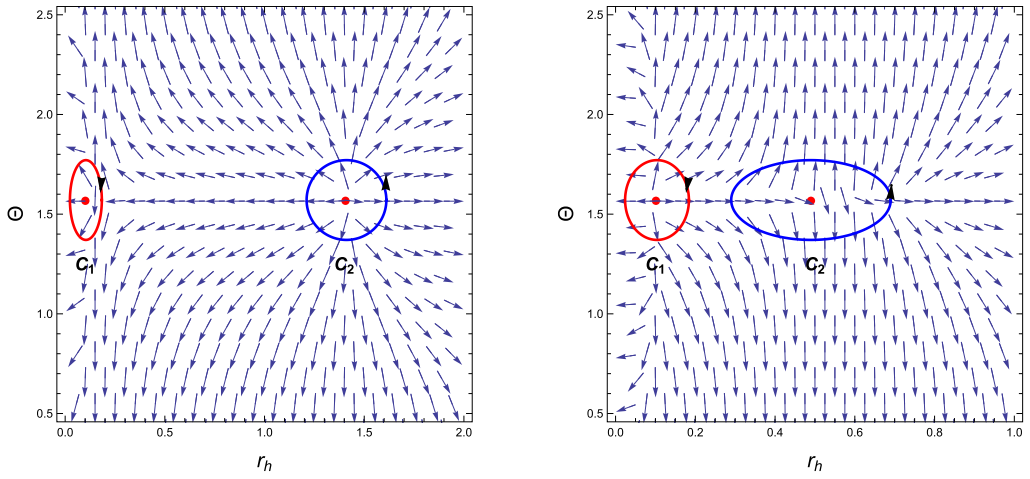


Fig. 7. (color online) Unit vector field n on the r_h–Θ plane for a four-dimensional Kerr–Sen AdS black hole with rotation parameter $a = 0.08$, pressure $P = 0.1193$, and dilatonic charge $b = 0.01$: (a) $\tau = \tau_{c1}$. The zero points (ZPs), marked by red dots, are located at $(r_h, \Theta) = (1.4208, \pi/2)$. The contours C_1 and C_2, enclosing the zero points, carry winding numbers $w_1 = 0$ and $w_2 = 1$, respectively; and (b) $\tau = \tau_{c2}$. The zero points (ZPs), marked by red dots, are located at $(r_h, \Theta) = (0.10122, \pi/2)$. C_1 and C_2 are two closed loops: C_1 encloses the zero point, whereas C_2 does not. The contours carry winding numbers $w_1 = 1$ and $w_2 = 0$, respectively. Their sum gives the total topological charge $W = 1$.

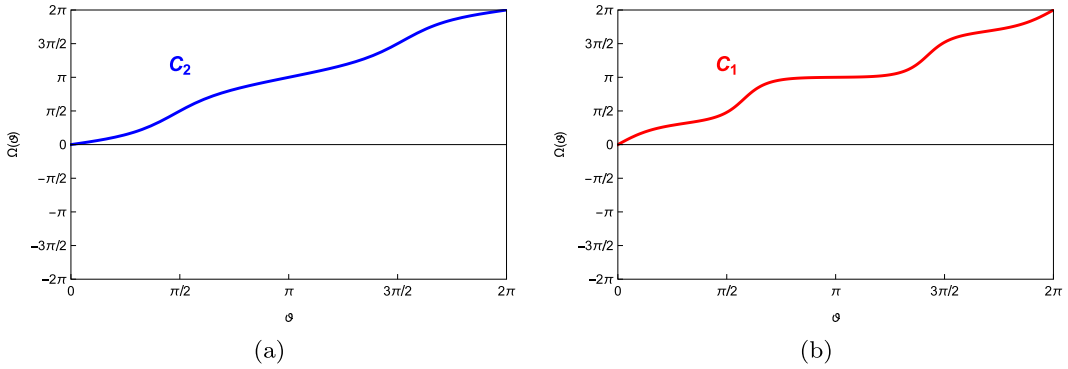


Fig. 8. (color online) Plots of Ω versus ϑ for contours C_1 (red solid curve) and C_2 (blue solid curve) for the Kerr–Sen AdS black hole. Panel (a) corresponds to Fig. 7(a), whereas panel (b) corresponds to Fig. 7(b).

contributions of the zero points canceling each other. A topological transition is indicated by the emergence of such a pair, in which zero points are created or annihilated while preserving the total topological charge.

Figure 7 and Fig. 8 show the topological nature of the thermodynamic phase structure of the Kerr–Sen AdS black hole. At the critical values $\tau = \tau_{c1}$ and $\tau = \tau_{c2}$, isolated zero points (ZPs) emerge in the vector field, signaling thermodynamic criticality. Although the location of the zero point shifts from the large-r_h regime to the small-r_h regime as τ varies, the total topological number remains invariant and is equal to $W = 1$. This invariance demonstrates that the phase transition is topological in origin and that the critical behavior is protected against smooth deformations of the thermodynamic parameters.

Next, we consider the case in which the negative cosmological constant vanishes, *i.e.*, $\Lambda = 0$. The plot in Fig. 9 shows the distribution of the unit vector field n on the $(r_h - \Theta)$ plane of a four-dimensional Kerr-Sen black hole with ensemble temperature $\tau = 3.3$ in the off-shell configuration. The rotation and dilaton charge parameters are set to $a = 0.08001$ and $b = 0.01$. The ZPs, marked by red dots and enclosed by the contours C_1 and C_2, are located

Table 1. The arrow directions along the four segments I_1–I_4 and the corresponding topological number w for each configuration.

	I_1	I_2	I_3	I_4	w
Case I	←	↑	→	↓	+1
Case II	←	↑	←	↓	0
Case III	→	↑	←	↓	−1
Case IV	→	↑	→	↓	0

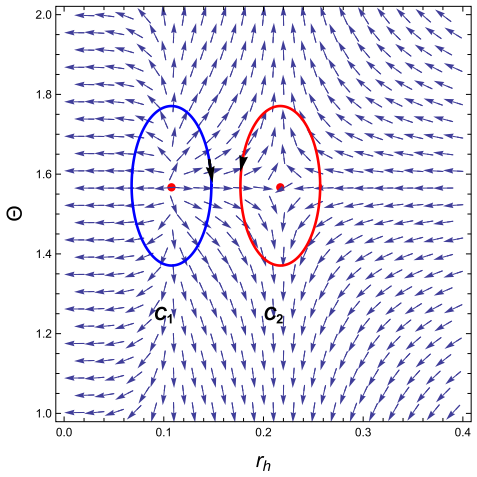


Fig. 9. (color online) The plot shows the unit vector field n on the r_h–Θ plane for a four-dimensional Kerr-Sen black hole with $\tau = 3.3$ and $a = 0.08001$. The zero points (ZPs), marked by red dots, are located at $(r_h, \Theta) = (0.107715, \pi/2)$ and $(0.216858, \pi/2)$. The orientations of the contours C_1 and C_2 are clockwise and anticlockwise, corresponding to the topological charges $Q_{c_1} = +1$ and $Q_{c_2} = -1$, respectively. The sum of the total topological charge is $Q_{\text{total}} = 0$.

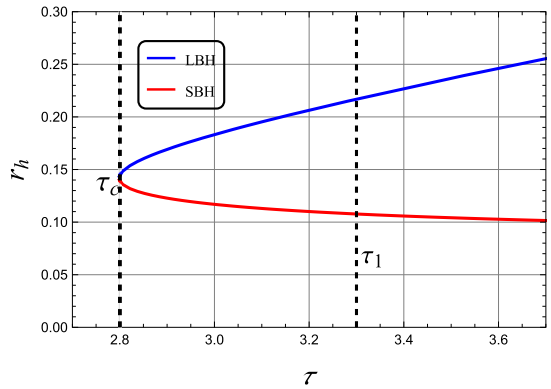


Fig. 10. (color online) The plot shows the stable and unstable black hole branches, in blue and red, respectively, for the Kerr–Sen black hole at $a = 0.08$ and $b = 0.01$. The blue and red curves correspond to the large black hole (LBH) and small black hole (SBH), respectively.

at $(r_h, \Theta) = (0.107715, \pi/2)$ and $(0.216858, \pi/2)$. Considering the orientations of the contours, C_1 and C_2 are clockwise and anticlockwise, respectively. Accordingly, the contours C_1 and C_2 correspond to topological charges $Q_{C_1} = +1$ and $Q_{C_2} = -1$, respectively. This yields the total topological charge $Q_{\text{total}} = 0$. On the other hand, in Fig. 10 we demonstrate the zero points of the component ϕ^{r_h} in the $(r_h - \tau)$ plane for the Kerr-Sen black hole with the fixed rotation and dilaton charge parameters $a = 0.08$ and $b = 0.01$. At $\tau = \tau_1$, there are two intersection points for the Kerr-Sen black hole. This behavior is similar to that in the RN and Kerr black hole configurations. At the intersection points, the condition $\tau = 1/T$ holds, and hence we obtain on-shell black hole solutions. Evidently, the intersection points coincide when $\tau = \tau_c$, and they vanish when $\tau < \tau_c$. One can easily check that at $\tau = \tau_c$, we have $\frac{\mathrm{d}^2\tau}{\mathrm{d}r_h^2} > 0$, indicating a creation point. The creation point at $\tau = \tau_c$ is responsible for the partition of the Kerr-Sen black holes into upper and lower branches, with corresponding winding numbers $w = -1$ and $w = +1$, respectively.

We summarize our discussion as follows. We emphasize that the limiting procedures are performed while keeping the thermodynamic ensemble fixed in the extended phase space. The conserved charges, including the electric charge, remain unchanged, whereas only the rotation parameter (a) or cosmological constant (Λ) is varied continuously. We explain that setting $a = 0$ removes the rotational degrees of freedom and reduces the system to the GMGHS AdS black hole. Consequently, the intermediate black hole branch disappears, leaving only two thermodynamic branches with opposite winding numbers, whose cancellation gives the total topological charge $W = 0$. Similarly, taking the asymptotically flat limit ($\Lambda = 0$) removes the AdS contribution responsible for the richer van der Waals phase structure. The resulting Kerr–Sen black hole therefore possesses only two thermodynamic branches with opposite winding numbers, again yielding $W = 0$. We further compare these results with the previously known topological classifications of Schwarzschild-AdS, RN-AdS, Kerr, and Kerr-AdS black holes, showing that the Kerr–Sen AdS black hole belongs to the same topological class ($W = 1$) as Kerr-AdS and RN-AdS, whereas the two limiting cases belong to the class with vanishing total topological charge.

Further, in Fig. 11, we illustrate the calculation of the topological number by plotting $\Omega(\vartheta)$ for the contours in Fig. 9. As the contours C_1 and C_2 do not intersect, the ZPs are topologically protected. The opposite orientations of these contours imply winding numbers with opposite signs. While the red solid curve in Fig. 11 carries the negative topological charge, the blue solid curve rep-

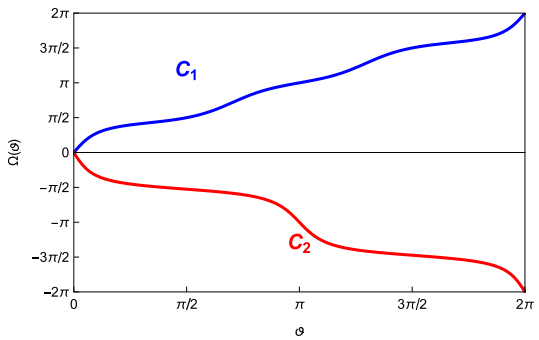


Fig. 11. (color online) The plot of Ω versus ϑ for the contours C_2 (red curve) and C_1 (blue solid curve) for $\Lambda = 0$.

resents the positive topological charge. Thus, the total topological charge is zero.

III. KERR–SEN TOPOLOGY USING COMPLEX RESIDUE TECHNIQUES

In this section, we evaluate the topological number using the complex residue technique [25]. In this method, we need to determine the winding number (w_i) for each pole obtained from the residue calculation. By summing the winding numbers associated with these poles, we obtain the total topological charge. Motivated by this approach, we first solve $\partial_{r_h}\mathcal{F}=0$ to obtain the expression for τ as a function of the horizon radius

$$\tau=\mathcal{G}(r_h). \tag{28}$$

The next step is to express the horizon radius in terms of the complex variable z, such that [25, 35]

$$\tau(r_h\to z)=\mathcal{G}(z).$$

The substitution of the event horizon radius (r_h) with a complex variable z is intended to extend the real variable to the complex plane $\mathbb{C}$, where the complex number is given by $z=x+iy$ and $x,y\in\mathbb{R}$ are real variables. We aim to construct a two-dimensional parametric space in which a real contour can be defined. This contour must enclose the thermodynamic defects determined from the expressions for $\mathcal{G}(z)$.

We now define a characteristic complex function $\mathcal{R}(z)$ as follows

$$\mathcal{R}(z)\equiv\frac{1}{\tau-\mathcal{G}(z)}. \tag{29}$$

The characterized complex function $\mathcal{R}(z)$ is related to the generalized free energy. More specifically, the complex residue method arises as a byproduct of the contour integral of a rational complex function $\mathcal{R}(z)$ that is analytic except at the isolated singular points $z_1,z_2,\ldots,z_m$ in the interior of C. The contour C is a simple closed curve oriented counterclockwise. As usual, the complex analytic function is defined within and on the contour C. The residue theorem is then applied, followed by the computation of the integral of the function $R(z)$ over the path C_k surrounding z_k, which can be written as,

$$\oint_C\frac{\mathcal{R}(z)}{2\pi\mathrm{i}}\mathrm{d}z=\sum_{k=1}^{m}\mathrm{Res}\left[\mathcal{R}(z_k)\right]. \tag{30}$$

In this way, the topological defects previously defined by $\phi^{r_h}=0$ (as shown in Eq. (14)) on the real plane are transformed into isolated singular points of the rational complex function $\mathcal{R}(z)$ on the z-plane.

Since each singular point identified as a thermodynamic defect can now be enclosed by an arbitrary contour, and the rational function $\mathcal{R}(z)$ is analytic everywhere except at the singular points $z_1,z_2,\ldots,z_N$, our task is to evaluate the integral of $\mathcal{R}(z)$ using the residue theorem along each closed contour enclosing the corresponding singular point. As implied by the Cauchy-Goursat theorem, the integral of the complex function $\mathcal{R}(z)/2\pi i$ around a contour C encircling all the singular points can equivalently be expressed as the sum of the integrals of $\mathcal{R}(z)$ along the interior contours C_i enclosing z_i.

Subsequently, we can characterize the winding numbers by calculating the residues of the complex function $\mathcal{R}(z)$ at its poles, which correspond to the topological defects associated with the on-shell black hole configurations. In what follows, to determine the topological characteristics of these defects, we normalize the residue and thereby define the winding number w_i associated with the singular point $z=z_i$, such that [25]

$$w_i=\frac{\mathrm{Res}\mathcal{R}(z_i)}{|\mathrm{Res}\mathcal{R}(z_i)|}=\mathrm{sgn}[\mathrm{Res}\mathcal{R}(z_i)], \tag{31}$$

where $|\mathrm{Res}\mathcal{R}(z_i)|$ denotes the absolute value of the residue of the complex-valued function, i.e., $\mathrm{Res}\mathcal{R}(z_i)$. The quantity $\mathrm{sgn}(x)$ is known as the sign function and has the following properties

$$\mathrm{sgn}(x)=\begin{cases}+1, & x>0,\\ 0, & x=0,\\ -1, & x<0.\end{cases}$$

It is worth noting that all singular points of interest are real and therefore satisfy the condition $\mathrm{Res}\mathcal{R}(z_i)\in\mathbb{R}$. Therefore, the global topological number W of the black hole spacetime is determined as

$$W=\sum_i w_i. \tag{32}$$

This can be understood by applying the Cauchy–Goursat theorem, which states that the integral of a complex function over an exterior contour can be evaluated in terms of the integrals along simple closed contours enclosing the isolated singular points. Thus, we have

$$\oint_C\mathcal{R}(z)\mathrm{d}z=\sum_i\oint_{C_i}\mathcal{R}(z)\mathrm{d}z. \tag{33}$$

The complex residue technique provides an effective framework for classifying and analyzing various isolated

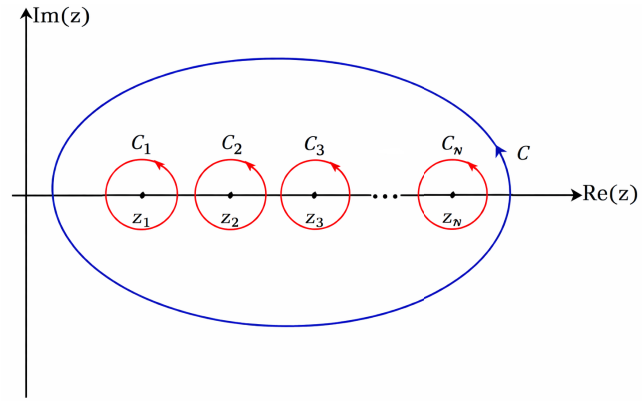


Fig. 12. (color online) A schematic diagram illustrating the contour integral of a function that is analytic everywhere except at a finite number of isolated singularities, $z_1, z_2, z_3, \ldots, z_N$, enclosed by a global contour C and a set of individual contours, $C_1, C_2, C_3, \ldots, C_N$, surrounding each singularity.

singular points. The contour plot of the analytic function could be derived using the complex residue techniques which is demonstrated schematically in Fig. 12. Of particular interest, it enables the calculation of winding numbers for higher-order poles, which illustrate features such as creation, annihilation, and critical points. For example, for the Schwarzschild black hole, there exists only one singular point, and the global topological number is $W = -1$. By contrast, the Reissner–Nordström (RN) and Reissner–Nordström–Anti-de Sitter (RN–AdS) black holes exhibit phase transitions with topological numbers $W = 0$ and $W = 1$, respectively. These results are reported in Ref. [7]. In this work, we demonstrate the possibility of computing the thermodynamic topologies of Kerr-Sen black hole solutions.

When $\Lambda = 0$, the Kerr-Sen AdS black hole reduces to the Kerr-Sen (KS) black hole such that,

$$\Delta_r = r^2 + 2br + a^2 - 2mr, \tag{34}$$

The generalized off-shell free energy $\mathcal{F}$ of the Kerr-Sen black hole system, as given in Eq. (13), is expressed as

$$\mathcal{F} = \frac{(a^2 + 2br + r^2)(\tau - 2\pi r)}{2r\tau}. \tag{35}$$

As defined in Eq. (29), the characteristic rational complex function of the Kerr-Sen black hole is computed as follows:

$$\mathcal{R}_{\rm KS} = \frac{a^2 - z^2}{4\pi z^2(b+z) - (z^2 - a^2)\tau}. \tag{36}$$

Because the denominator is a cubic function of z, we can rewrite the above equation in the form

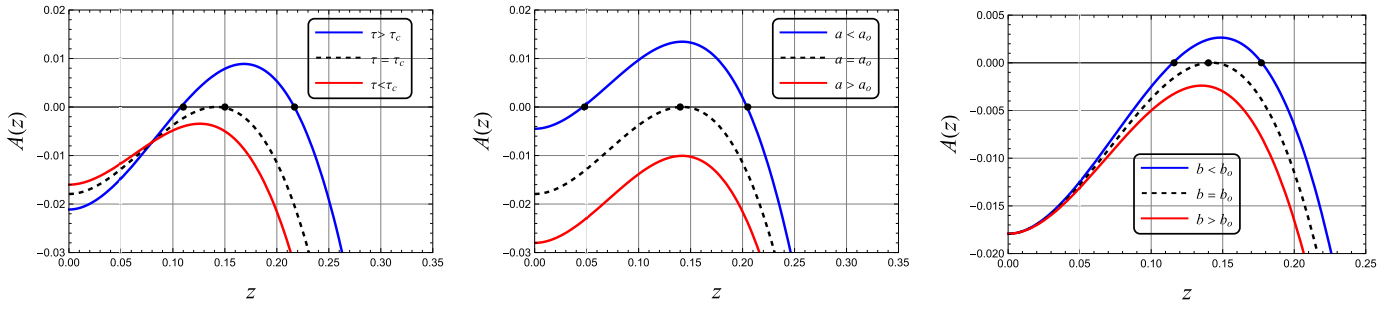
$$\mathcal{R}_{\rm KS}(z) = \frac{a^2 - z^2}{4\pi(z-z_1)(z-z_2)(z-z_3)} = \frac{a^2 - z^2}{\mathcal{A}(z)}, \tag{37}$$

where the polynomial function $\mathcal{A}(z)$ is given by

$$\mathcal{A}(z) = 4\pi z^2(b+z) - (z^2 - a^2)\tau. \tag{38}$$

We need to solve this polynomial by setting it equal to zero for different values of the parameters a, b, and τ. Once we solve for z, we can distinguish the winding numbers using Eq. (31).

In Fig. 13, we present plots of the complex polynomial $\mathcal{A}(z)$ for three different cases. Fig. 13(a) shows the behavior of $\mathcal{A}(z)$ for different values of the parameter τ with $a = 0.08$ and $b = 0.01$. There is only one pole for $\tau = \tau_c$, two poles for $\tau > \tau_c$, and no pole for $\tau < \tau_c$. For $\tau = \tau_c$, we have the large black hole branch, and the pole is located at $z = 0.141802$, as shown by the black dashed curve. The winding number corresponding to the pole at



(a) (b) (c)

Fig. 13. (color online) Roots of the polynomial equation $A(z) = 0$ for different values of the model parameters. Panels (a), (b), and (c) correspond to variations in the parameters τ, a, and b, respectively. The evolution of the roots illustrates how the solution structure depends on the underlying physical parameters.

$z = 0.141802$ is assigned as $w = +1$. For $\tau > \tau_c$, there are two poles located at $z_1 = 0.107716$ and $z_2 = 0.216858$, representing the small and large black hole phases, respectively. The corresponding winding numbers around the poles at z_1 and z_2 are $w_1 = -1$ and $w_2 = +1$. Hence, the global topological number is $W = w_1 + w_2 = 0$. For $\tau < \tau_c$, there is no pole and hence no topological charge. Similar situations are observed in Fig. 13(b) and Fig. 13(c), where we consider variations of the rotation parameter a and the dilaton charge parameter b, respectively, for a fixed value of τ. In Fig. 13(b), we show the single-pole ($a = a_0$), double-pole ($a > a_0$), and no-pole ($a < a_0$) cases for $\tau = 2.79857$. Similarly, in Fig. 13(c), we depict the single-pole, double-pole, and no-pole cases for $b = b_0$, $b > b_0$, and $b < b_0$, respectively, at fixed $\tau = 2.79857$.

We clarify that the residue formulation is mathematically equivalent to Duan's topological current approach with respect to the global topological classification. However, its significance extends beyond that of an alternative mathematical representation. The residue formulation naturally transfers the thermodynamic problem into the complex plane, where isolated thermodynamic defects become poles of a meromorphic function. Consequently, the winding numbers are obtained directly from the signs of the residues, the creation and annihilation of thermodynamic defects are interpreted as mergers or disappearances of poles, and higher-order poles provide a natural framework for analyzing degenerate critical points. This formulation provides a powerful machinery of complex analysis for studying thermodynamic topology.

Therefore, while both methods produce identical global topological charges, the residue approach offers a complementary analytical framework that yields a deeper mathematical understanding of thermodynamic defects and critical phenomena. We have revised the manuscript accordingly to make these conceptual advantages much clearer.

IV. CONCLUSION

Topology has emerged as a powerful tool for understanding black hole thermodynamics. By treating black hole phases as topological defects in a thermodynamic space, we can categorise them in a coordinate-independent manner, thereby revealing universal features that might otherwise remain hidden. The Kerr-Sen black hole provides a particularly interesting setting for exploring these ideas. It arises in string theory, rotates, and carries a dilaton charge —ingredients that could potentially alter the topological picture observed in simpler black holes. Motivated by this, we set out to determine how rotation and the dilaton field influence thermodynamic topology and whether the patterns established for Schwarzschild, Reissner-Nordström, and Kerr black holes still hold in this richer setting.

Indeed, we studied the thermodynamics of Kerr-Sen AdS black holes using two different approaches to understand their topological properties. The first method uses Duan's ϕ-mapping theory, while the second is a new technique based on complex residues. By examining the off-shell free energy and the vector field it generates in the parameter space (r_h, Θ), we investigated three versions of the black hole: the full Kerr-Sen AdS black hole, its non-rotating version called GMGHS AdS (where $a = 0$), and the flat-space version with no cosmological constant (where $\Lambda = 0$). We note that the Kerr-Sen AdS black hole exhibits three thermodynamic phases, viz., small, intermediate, and large black holes. These phases have winding numbers $+1$, -1, and $+1$, respectively. Their sum yields a total topological charge of $Q = +1$. This places the Kerr-Sen AdS black hole in the same topological family as the well-known Reissner-Nordström AdS and Kerr-AdS black holes. Interestingly, varying the dilaton charge b does not affect the total topological charge. This indicates that the dilaton field does not alter the basic topological character of the black hole. By contrast, the rotation parameter a plays a major role in shaping the phase structure and determining how many critical points appear. Thus, in the context of thermodynamic topology, spin is far more influential than the dilaton charge.

Examining the special cases also yielded interesting results. When rotation is turned off ($a = 0$) to obtain the GMGHS AdS black hole, the total topological charge becomes zero ($W = 0$). This occurs because the two phases have winding numbers $+1$ and -1, which cancel each other. The same behaviour appears for the flat Kerr-Sen black hole (with $\Lambda = 0$)—it also has $W = 0$, even though it exhibits two distinct phases. These results indicate that, although rotation and the cosmological constant do affect the topology, the dilaton charge does not change the overall topological picture. This suggests a degree of universality in the topological behaviour of black hole thermodynamics. One of the most interesting aspects of this work is the new complex residue method we employed. Instead of using Duan's approach, we extended the thermodynamic functions into the complex plane. We constructed a complex function $\mathcal{R}(z) = 1/\tau - \mathcal{G}(z)$ and found that its singular points coincide exactly with the thermodynamic defects. The residues at these points yield the winding numbers through the simple formula $w_i = \mathrm{sgn}[\mathrm{Res}\mathcal{R}(z_i)]$. This provides a much cleaner mathematical framework while yielding the same results as Duan's method. It also offers a fresh perspective on critical points and may help us understand phenomena such as creation and annihilation events in phase transitions.

When we examined the complex polynomial $\mathcal{A}(z) = 4\pi z^2(b+z) - (z^2 - a^2)\tau$ for the flat-space Kerr-Sen black hole, we found three distinct situations. At the critical

temperature $\tau = \tau_c$, there is only one pole. For temperatures above τ_c, there are two poles corresponding to small and large black hole phases with winding numbers -1 and $+1$. For temperatures below τ_c, there are no poles at all. We observed similar patterns when varying the rotation parameter a and the dilaton charge b. This shows that the topological classification is quite robust and that the complex residue method works very well in capturing the relevant features of black hole thermodynamics. Our results point to several broader implications. First, the fact that the dilaton charge does not change the total topological charge suggests that this topological classification may be a universal feature of black hole thermodynamics and may be insensitive to certain details such as matter couplings. Second, the agreement between the two methods is reassuring and improves our mathematical understanding of the meaning of thermodynamic defects. Third, the use of complex analysis in black hole thermodynamics opens new possibilities, as it allows powerful tools from complex analysis to be applied to the study of phase transitions.

Looking ahead, there is much more to explore. For example, we could investigate how the thermodynamic topology studied here connects with holographic dual field theories. This might help us understand how topological behaviour in gravity manifests as distinct phases in field theories. We could also extend these ideas to non-equilibrium situations, such as black hole formation, evolution, or evaporation over time. Another interesting question is whether the topological patterns we have identified are universal, that is, whether they also appear in other black hole solutions arising from string theory or higher-curvature gravity. Finally, a deeper investigation of the topology may provide hints about the microscopic structure of black holes and about what they can reveal regarding the deeper nature of quantum gravity.

To wrap up, this work shows that topological methods provide deep insights into black hole phase transitions. They offer a coordinate-independent way of viewing the problem and reveal universal features of black hole thermodynamics. The complex residue method, in particular, is both powerful and elegant. It complements existing approaches and could be highly useful for future studies on the role of topology in quantum gravity and holography.

An interesting extension of the present work is to explore the thermodynamic topology of Kerr-Sen AdS black holes by interpreting their equilibrium states as topological defects in the parameter space of extended phase-space thermodynamics. Such an investigation may reveal novel topological classes or subclasses [47], thereby enriching the existing topological classification and providing deeper insights into the thermodynamic evolution, stability, and phase structure of rotating charged AdS black holes.

ACKNOWLEDGEMENTS

The authors would like to thank the Inter-University Centre for Astronomy and Astrophysics (IUCAA), Pune, for its hospitality while part of this work was being carried out.

References

[1] B. P. Abbott *et al.* (LIGO Scientific and Virgo Collaborations), Phys. Rev. Lett. **116**(24), 241102 (2016)
[2] B. P. Abbott *et al.* (LIGO Scientific and Virgo Collaborations), Phys. Rev. Lett. **116**(24), 241103 (2016)
[3] K. Akiyama *et al.* (Event Horizon Telescope Collaboration), Astrophys. J. Lett. **875**(1), L6 (2019)
[4] K. Akiyama *et al.* (Event Horizon Telescope Collaboration), Astrophys. J. Lett. **930**(2), L12 (2022)
[5] P. V. P. Cunha, E. Berti, and C. A. R. Herdeiro, Phys. Rev. Lett. **119**(25), 251102 (2017)
[6] P. V. P. Cunha and C. A. R. Herdeiro, Phys. Rev. Lett. **124**(18), 181101 (2020)
[7] S. W. Wei, Y. X. Liu, and R. B. Mann, Phys. Rev. Lett. **129**(19), 191101 (2022)
[8] S. W. Wei and Y. X. Liu, Phys. Rev. D **105**(10), 104003 (2022)
[9] M. Rehan, S. Ul Islam, and S. G. Ghosh, Sci. Rep. **14**(1), 13875 (2024)
[10] J. M. Bardeen, B. Carter, and S. W. Hawking, Commun. Math. Phys. **31**, 161 (1973)
[11] S. W. Hawking, Nature **248**, 30 (1974)
[12] S. W. Hawking, Commun. Math. Phys. **43**, 199 (1975) [Erratum: Commun. Math. Phys. **46**, 206 (1976)]
[13] S. W. Hawking and D. N. Page, Commun. Math. Phys. **87**, 577 (1983)
[14] R. Li and J. Wang, JHEP **12**, 208 (2021)
[15] R. Li and J. Wang, JHEP **05**, 128 (2022)
[16] C. h. Liu, R. Li, K. Zhang *et al.*, JHEP **11**, 068 (2023)
[17] R. Li, K. Zhang, and J. Wang, Phys. Rev. D **104**(8), 084060 (2021)
[18] R. Li and J. Wang, Phys. Rev. D **108**(4), 044057 (2023)
[19] Y. S. Duan and M. L. Ge, Sci. Sin. **9**(11), 1072 (1979)
[20] A. Das and J. Maharana, Mod. Phys. Lett. A **16**(38), 2483 (2001)
[21] L. B. Fu, Y. S. Duan, and H. Zhang, Phys. Rev. D **61**, 045004 (2000)
[22] S. W. Wei and Y. X. Liu, Phys. Rev. D **107**(6), 064006 (2023)
[23] P. K. Yerra, C. Bhamidipati, and S. Mukherji, Phys. Rev. D **106**(6), 064059 (2022)
[24] J. Sadeghi, S. N. Gashti, M. R. Alipour *et al.*, Annals Phys. **455**, 169391 (2023)
[25] C. x. Fang, J. Jiang, and M. Zhang, JHEP **01**, 102 (2023)
[26] Y. T. Liu, C. F. Guan, C. Du *et al.*, Symmetry **15**(3), 643 (2023)
[27] N. C. Bai, L. Li, and J. Tao, Phys. Rev. D **107**(6), 064015 (2023)

[28] M. S. Ali, H. El Moumni, J. Khalloufi *et al*., Annals Phys. **465**, 169679 (2024)
[29] D. Wu, Phys. Rev. D **107**(2), 024024 (2023)
[30] D. Wu and S. Q. Wu, Phys. Rev. D **107**(8), 084002 (2023)
[31] D. Wu, S. Q. Wu, P. X. Wu *et al*., Phys. Rev. D **103**(4), 044014 (2021)
[32] M. S. Ali, S. G. Ghosh, and A. Z. Wang, Phys. Rev. D **108**(4), 044045 (2023)
[33] Z. Y. Gao, X. Q. Kong, and L. Zhao, Eur. Phys. J. C **82**(2), 112 (2022)
[34] D. Wu, P. X. Wu, H. W. Yu, and S. Q. Wu, Rev. D **102**(4), 044007 (2020)
[35] B. Hazarika and P. Phukon, Nucl. Phys. B **1012**, 116837 (2025)
[36] S. W. Wei, Y. X. Liu, and R. B. Mann, Phys. Rev. D **100**(12), 124033 (2019)
[37] S. W. Wei and Y. X. Liu, Phys. Rev. Lett. **115**, 111302 (2015) [Erratum: Phys. Rev. Lett. **116**, 169903 (2016)]
[38] S. W. Wei, Y. X. Liu, and R. B. Mann, Phys. Rev. Lett. **123**(7), 071103 (2019)
[39] A. N. Kumara, C. L. A. Rizwan, K. Hegde *et al*., Phys. Rev. D **103**(4), 044025 (2021)
[40] J. Sadeghi, M. A S. Afshar, S. N. Gashti *et al*., Phys. Scripta **99**(2), 025003 (2024)
[41] C. H. Liu and J. Wang, Phys. Rev. D **107**(6), 064023 (2023)
[42] W. T. Liu, L. Zhang, D. Wu *et al*., Class. Quant. Grav. **42**, 125007 (2025)
[43] A. Sen, Phys. Rev. Lett. **69**, 1006 (1992)
[44] N. Wu, M. Baggioli, and W. J. Li, JHEP **05**, 014 (2021)
[45] Y. S. Duan, S. Li, and G. H. Yang, Nucl. Phys. B **514**, 705 (1998)
[46] S. W. Wei, Phys. Rev. D **102**(6), 064039 (2020)
[47] D. Wu, W. T. Liu, S. Q. Wu *et al*., Phys. Rev. D **111**(6), L061501 (2025)